Capillary Waves at the Liquid−Vapor Interface. Widom−Rowlinson Model at Low Temperature

Frank H. Stillinger*

AT&T Bell Laboratories, Murray Hill, New Jersey 07974

John D. Weeks

Institute for Physical Science and Technology and Department of Chemistry, University of Maryland, College Park, Maryland 20742

Received: July 5, 1994; In Final Form: August 18, 1994[⊗]

We have examined in detail the structure and properties of the liquid−vapor interface for the two-dimensional Widom−Rowlinson model in its low-temperature regime. Various simplifying features permit the deduction of several basic results. Included among these are (1) unambiguous definition of capillary wave modes with upper wavelength cutoff proportional to $\varrho_l^{-1/3}$ (ϱ_l = liquid density); (2) wavelength dispersion of bare surface tension; and (3) nonmonotonic intrinsic density profile (i.e., that with vanishing capillary wave amplitudes). In an Appendix we show how many of these results can be extended to the three and higher dimensional cases.

I. Introduction

The structure and properties of liquid−vapor interfaces have drawn serious scientific attention for nearly two centuries.[1] Even so, the subject still elicits clever experiments[2−8] and lively theoretical discourse.[9−15] The present paper focuses on a conceptually simple model for liquid−vapor coexistence, innovated by Widom and Rowlinson,[16−18] which in its two-dimensional version becomes sufficiently tractable analytically to yield some new insights for the interface problem.

The matter distribution at the interface between coexisting liquid and vapor phases varies continuously with position, smoothly connecting the high bulk density of the former to the low bulk density of the latter. The first serious attempt at quantitative description of this interfacial density profile must be attributed to van der Waals;[19−20] subsequent refinements have included a formulation to account for "nonclassical" critical point singularities.[9] The van der Waals intrinsic density profile displays a finite characteristic width at all temperatures below critical, though this width diverges as the critical point is approached. External forces, such as gravity, play no direct role in the van der Waals theory for the planar liquid−vapor interface.

More recently it has been recognized[21] that collective surface excitations in the form of capillary waves should be an important ingredient in a comprehensive and accurate description of the liquid−vapor interface. In particular, for the planar interface long-wavelength capillary wave modes become unstable as the gravitational field strength goes to zero, with the result that even well below the critical temperature the interface mean-square width diverges (logarithmically) in that zero-field limit. Although the original capillary wave model was phenomenological, rather than rigorously derived from fundamental principles of many-body statistical physics, its basic idea seems to have received support both from experiment[2,3,5−8] and from exact calculations with the two-dimensional Ising model.[22]

Both the van der Waals and the capillary wave approaches capture important aspects of the interface problem, but neither represents a complete description. Consequently several proposals to combine basic features of the two have now appeared.[11,15,23] This is an attractive prospect, but it is not free of ambiguity: uncertainties remain regarding the number of capillary wave modes, and how they interact with, and modify, the remaining degrees of freedom that constitute the "van der Waals part" of the interface problem. Helping to resolve these ambiguities is our primary motivation in the present study.

Section II defines the two-dimensional version of the Widom−Rowlinson (WR) model. Section III discusses its liquid−vapor coexistence, focusing on the low-temperature regime to which the subsequent analysis is restricted. Section IV shows that a distinguished set of interface particles provides a natural description of the models' liquid surface, and their positions define capillary waves. This permits us to define the intrinsic density profile at low temperature in a precise and natural way (section V); studying this limit may provide insight into more general situations, where other characterizations of the "intrinsic profile" may seem equally natural, but whose precise definition remains surrounded with some element of ambiguity.[11] Section VI examines the wavelength dependence of bare (unrenormalized by capillary waves) surface tension. Section VII offers a discussion of several issues, including implications of present results for the general theory of liquid−vapor interfaces. An Appendix indicates how the principal results can be extended to the Widom−Rowlinson model in three (or more) dimensions.

II. WR Model in Two Dimensions

The original presentation of the WR model concentrated primarily on the three-dimensional case, with a few exact results quoted for the one-dimensional version.[16] Subsequent studies have only considered three dimensions.[17,18] We now examine the two-dimensional case for this classical continuum model.

Each of the structureless particles in the WR model sits at the center of a disk with radius R. The potential energy function Φ for an arbitrary configuration $\mathbf{r}_1...\mathbf{r}_N$ of N particles in the plane is assigned the value

$$\Phi(\mathbf{r}_1...\mathbf{r}_N) = (\epsilon/a)[A_c(\mathbf{r}_1...\mathbf{r}_N) - Na] \qquad (2.1)$$

where $\epsilon > 0$ is the basic energy unit in the model, $a = \pi R^2$ is the disk area, and A_c is the area in the plane covered by the N disks in the given configuration. Obviously A_c can be as large as Na if no pair of disks is close enough to overlap, but it attains its absolute minimum a if all particles are coincident.

[⊗] Abstract published in *Advance ACS Abstracts*, February 1, 1995.

0022-3654/95/2099-2807$09.00/0

Consequently Φ has the following bounds:

$$-(N-1)\epsilon \leq \Phi \leq 0 \tag{2.2}$$

This suffices to assure that the thermodynamic limit exists for the model.[24] The various thermodynamic properties of interest then can be extracted, for example, from the canonical partition partition function

$$Z_N(\beta) = (\lambda^{2N}N!)^{-1} \int \mathrm{d}\mathbf{r}_1 \ldots \int \mathrm{d}\mathbf{r}_N \exp[-\beta(U+\Phi)] \tag{2.3}$$

where $\beta = (k_B T)^{-1}$, λ is the mean thermal deBroglie wavelength, and $U(\mathbf{r}_1 \ldots \mathbf{r}_N)$ is the potential of external forces (if any) acting on the system.

Although Φ in eq 2.1 has an elementary geometric interpretation, it is not a "simple" interaction potential in the conventional sense. It consists of a sum of the type

$$\Phi(1\ldots N) = \sum_{n=2}^{N} \sum_{i_1 \ldots i_n} v_n(i_1 \ldots i_n) \tag{2.4}$$

where each n-body interaction v_n can be expressed as a linear combination of A_c's for n or fewer particles.

We note in passing that the one-component WR model just defined can be transformed exactly into a symmetrical two-component system in which only two-body interactions operate. This implies that a basic underlying symmetry exists hidden within the starting one-component model with its nonadditive interactions.[16] However, that symmetry plays no direct role in our present study.

The continuous attractive forces between particles generated by Φ, eq 2.1, suffice to produce a liquid−vapor phase transition at sufficiently low temperature, as discussed in section III. This feature alone confers significance upon the WR model. Its major shortcoming, however, is the absence of even weakly repelling particle cores, and for that reason it cannot crystallize at any temperature. However, for our purposes here this shortcoming is actually a virtue. It allows us to examine properties of the model at very low temperatures, where description both of the bulk phases and of the interface structure is especially simple. The temperature acts as a natural small parameter, permitting an analysis of this continuum model in a way that complements the low-temperature analysis of the interface in a lattice gas (Ising model).[22]

III. Low-T Particle Distribution

Since the space dimension exceeds 1, the mean field approximation supplies a reliable qualitative guide to the bulk thermodynamic behavior of the WR model. Application of this approximation is a standard statistical mechanical procedure,[25,26] so we shall simply quote a few results relevant to the present study.

The principal mean field result for the two-dimensional WR model is the presence of liquid−vapor coexistence at all temperatures below a critical point located at

$$(Na/A)_{cr} = 1$$

$$(\beta\epsilon)_{cr} = e \tag{3.1}$$

The critical density specified by the first of these conforms to the exact hidden symmetry alluded to earlier[16] and is therefore itself to be regarded as an exact result. The second of eqs 3.1, however, is only a mean field estimate of the true critical temperature.

The mean field approximation yields a "classical" critical point with associated thermodynamic singularities of the van der Waals type. A more precise treatment of the WR model critical point is expected to yield "nonclassical" critical point singularities that fall within the Ising model universality class.[27] Since the mean field approximation also erroneously assigns a "classical" critical point to the two-dimensional Ising model, it seems reasonable to suppose that generally it mistreats the WR and Ising models in roughly parallel fashion. On this basis the known ratio of mean field to exact critical temperatures for the two-dimensional Ising model[28] can be used to revise the second of eqs 3.1:

$$(\beta\epsilon)_{cr} \cong 4.79 \tag{3.2}$$

Of course this is only an estimate; it would be desirable to have an accurate direct determination.

As temperature declines below critical, the densities of coexisting liquid and vapor become less and less alike. In the low-temperature regime the mean field approximation specifies that those densities have the following asymptotic forms:

$$\varrho_l \cong \beta\epsilon/a$$

$$\varrho_v \cong (\beta\epsilon/a)\exp(-\beta\epsilon) \tag{3.3}$$

which respectively grow without bound and converge to zero. That ϱ_l becomes so large is another consequence of the absence of repelling particle cores. The Boltzmann factor driving ϱ_v to zero in the low-temperature limit reflects the increase in covered area by one disk as a particle is transferred from dense liquid into substantially empty space (dilute vapor).

Results (3.3) lead to the observation that at low temperatures the interior of both liquid and vapor phases dynamically have the character of ideal gases, with particles moving along linear trajectories substantially without collisions. This is obvious for the extremely dilute vapor. Within the dense liquid virtually all points are covered simultaneously by many disks, so Φ remains invariant to the motion of any one disk, implying no force on that disk. For these reasons, the mean field results (3.3) should be asymptotically correct at low temperature. In the Appendix we rederive (3.3) using this ideal gas description of the bulk partition functions.

With fixed particle number N and system area A, a temperature reduction sufficiently far below critical will always cause phase separation into an adjoining pair of macroscopic phases, the positions and shapes of which depend on the external forces present. We can assume in the following that a weak gravitational field is present only to localize the liquid and vapor phases and to produce a macroscopically flat interface between them.

Suppose that the centers of the N_l particles comprising the dense low-temperature liquid are confined to the liquid-phase area $A_l \leq A$, whose boundary has length L_0.

$$A_l = \varrho_l N_l \tag{3.4}$$

Particles at or near the boundary have disks extending beyond that boundary. Because ϱ_l is large, the covered area will extend with negligible error a full strip of width R beyond the boundary, as Figure 1 illustrates. Provided the region A_l remains convex, it is easy to show that the extended region covered by liquid-phase disks is

$$A_l + L_0 R + O(1) \tag{3.5}$$

This, in connection with the WR potential function eq 2.1, implies that the excess potential energy per unit length of flat

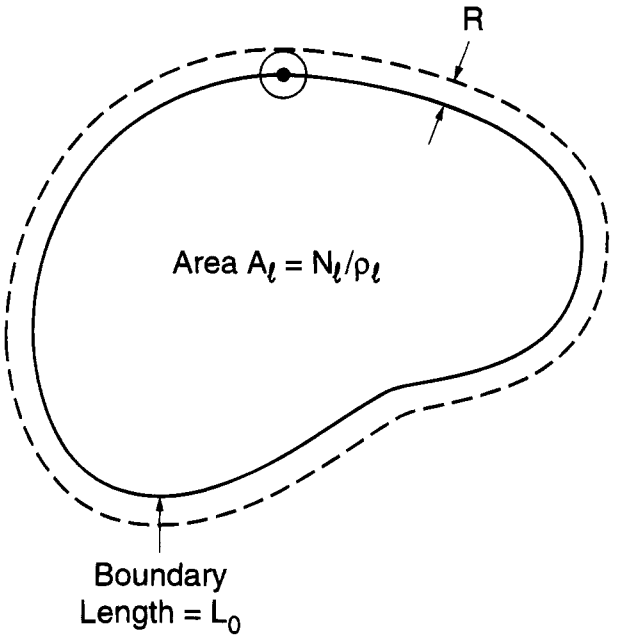

Figure 1. Schematic illustration of area A_l occupied by the dense low-temperature liquid. Particle centers are confined by the length L_0 boundary.

boundary, or surface tension γ_0 at $T = 0$, is given by

$$\Delta\Phi/L_0 \equiv \gamma_0 = \epsilon/(\pi R) = \epsilon R/a \tag{3.6}$$

Note that the surface tension remains bounded and behaves quite normally at $T \to 0$ despite the divergence of the bulk liquid density in (3.3).

IV. Capillary Waves

We now examine the structure of the liquid surface in detail. By confining attention to the low-temperature regime $\beta \gg \beta_c$, we can consistently assume that the vapor density vanishes, *i.e.* $N_l \cong N$.

First observe that the particles of the liquid phase fall into two sets, "surface" particles and "bulk" particles. Their numbers vary with configuration but in all cases will be denoted by N_s and N_b, respectively. Surface particles are those whose disks contribute circular arcs to the outer boundary of A_c, the region covered by liquid-particle disks. Bulk particles are all the rest; they are the ones moving along linear trajectories within the liquid's gapless interior, eventually to encounter and scatter from the surface.

Figure 2 illustrates a group of surface particles that contribute a section of the outer boundary of the liquid-phase A_c. The circular arcs whose union determines that outer boundary have been darkened for emphasis. Note also the presence of an inner boundary (dashed line in Figure 2) below which the center of a bulk particle must stay in order to remain a bulk particle. This inner boundary consists of radius R circular arcs, centered at cusps of the outer boundary, and passing through centers of surface particles.

Figure 2 shows the possibility of a surface protrusion, specifically a single surface particle sitting atop another surface particle. It is distinguished by the fact that the inner boundary limiting bulk particle positions does not pass through its center. Consequently, its presence does not increase the configurational freedom of the N_b bulk particles; but creating such a protrusion involves expenditure of an excitation energy of order ϵ. Similar observations apply to larger protrusions in the form of longer particle chains attached at one end to the liquid phase. A chain of particles attached at both ends (a "handle") amounts to a gap in the bulk liquid, which we have argued above is a negligible occurrence. As a result of these considerations the concentration of all protrusions must vanish exponentially as temperature goes to zero.

Consequently, the configuration of the surface particles is simple in the sense that they present an uninterrupted and unbranched chain from left to right. Furthermore, in this low-temperature regime where the interior of the liquid is dense and gapless, the WR potential function Φ, eq 2.1, depends only on the surface particle positions $\mathbf{r}_1 \ldots \mathbf{r}_{N_s}$. Let A_b be the area available to each of the N_b bulk particles when the surface set is in place. We can now write the canonical partition function Z_N, eq 2.3, for the low-temperature WR model in two dimensions as follows ($N_b = N - N_s$):

$$Z_N(\beta) \cong \lambda^{-2N} \sum_{N_b} (N_b!)^{-1} \int d\mathbf{r}_1 \ldots \int d\mathbf{r}_{N_s} \times \exp[-\beta\Phi(\mathbf{r}_1 \ldots \mathbf{r}_{N_s})][A_b(\mathbf{r}_1 \ldots \mathbf{r}_{N_s})]^{N_b} \tag{4.1}$$

Here we assume that the identical surface particles are serially

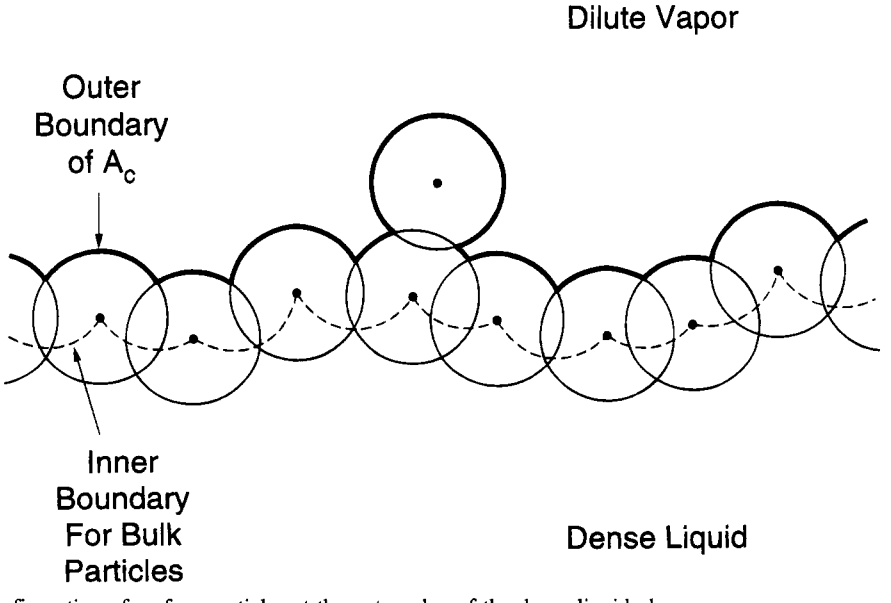

Figure 2. Illustrative configuration of surface particles at the outer edge of the dense liquid phase.

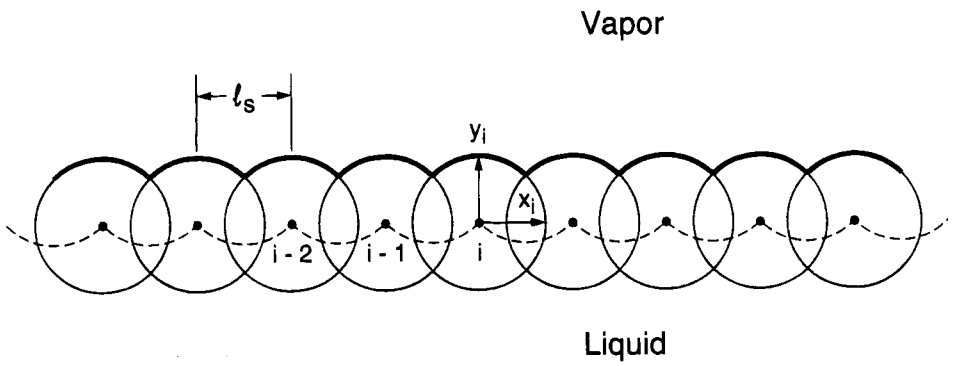

Figure 3. Regular reference configuration of surface particles. Coordinates x_i, y_i measure displacement of particle i from its reference site.

ordered (say from left to right), and of course the integrations must observe that ordering and be consistent with the definition of surface particles. Although expression 4.1 contains a sum over N_b, or equivalently N_s, we expect dominance by the neighborhood of a maximum term, to be determined below.

In order to facilitate further analysis, it will be convenient to refer the positions of the surface particles to a locally linear and periodic array of reference sites. These are depicted in Figure 3. If L_0 is the nominal interface length, the horizontal spacing between successive sites will be

$$l_s = L_0/N_s \tag{4.2}$$

General configurations of surface particles will be specified by sets of displacements x_i, y_i for every particle i from its reference site, respectively giving tangential and normal components (see Figure 3). We can require that the area $A_b^{(0)}$ available to bulk particles when all surface particles are at their reference sites has the value required by the liquid density ϱ_l in eq 3.3:

$$A_b^{(0)} = N_b/\varrho_l = N_b a/\beta\epsilon \tag{4.3}$$

The total covered area in this reference configuration, $A_c^{(0)}$, is larger of course; one readily finds

$$A_c^{(0)} = A_b^{(0)} + N_s R^2 \arccos[1 - l_s^2/(2R^2)] \tag{4.4}$$

As surface particles stray from their reference sites, we have area changes

$$A_b(\mathbf{r}_1 \ldots \mathbf{r}_{N_s}) = A_b^{(0)} + \delta A_b(\mathbf{r}_1 \ldots \mathbf{r}_{N_s}) \tag{4.5}$$

and

$$A_c(\mathbf{r}_1 \ldots \mathbf{r}_{N_s}) = A_c^{(0)} + \delta A_c(\mathbf{r}_1 \ldots \mathbf{r}_{N_s}) \equiv (a/\epsilon)\Phi(\mathbf{r}_1 \ldots \mathbf{r}_{N_s}) + Na \tag{4.6}$$

Then since

$$[A_b]^{N_b} = \left(\frac{aN_b}{\beta\epsilon}\right)^{N_b}\left[1 + \frac{\beta\epsilon\delta A_b}{aN_b}\right]^{N_b} \cong \left(\frac{aN_b}{\beta\epsilon}\right)^{N_b} \exp\left(\frac{\beta\epsilon\delta A_b}{a}\right) \tag{4.7}$$

the canonical partition function Z_N, eq 4.1, can be put into the following form:

$$Z_N \cong \lambda^{-2N} \exp(\beta\epsilon N) \sum_{N_b}\left(\frac{a}{\beta\epsilon}\right)^{N_b} \times \exp\left[-\frac{\beta\epsilon R^2 N_s}{a}\arccos\left(1 - \frac{l_s^2}{2R^2}\right)\right] \int d\mathbf{r}_1 \ldots d\mathbf{r}_{N_s} \times \exp\left[\frac{\beta\epsilon}{a}(\delta A_b - \delta A_c)\right] \tag{4.8}$$

Here we have used Stirling's approximation for $N_b!$, with neglect of the thermodynamically insignificant factor $(2\pi N_b)^{1/2}$. Just as before, the integrals in eq 4.8 must only involve configurations that are consistent with the surface particle definition, and with the serial ordering along the interface.

The difference $\delta A_c - \delta A_b$ represents the change, with surface particle displacements, of the area between the two scalloped curves shown in Figure 3, each of which is composed of radius R circular arcs. Figure 4 indicates that this area generally can be resolved into a sequence of circular sectors whose vertices alternate between the inner and outer curves.

Since present interest concerns the nominally flat interface, it is feasible and convenient to suppose that periodic boundary conditions apply in the horizontal direction. In other words, the interface has macroscopic period L_0, returning to its original height and configuration after wandering through intervening surface fluctuations. With this horizontal periodicity imposed, it is easy to establish that the total area of all circular sectors whose vertices lie on the outer (vapor side) curve exactly equals the total area of all circular sectors whose vertices lie on the inner (liquid side) curve. Furthermore, the area of any sector is proportional to its vertex angle, and all sectors have radius R. In view of these facts, one finds

$$\delta A_c - \delta A_b = R^2 \sum_{i=1}^{N_s} \times \left[\arccos\left(1 - \frac{l_i^2}{2R^2}\right) - \arccos\left(1 - \frac{l_s^2}{2R^2}\right)\right] \tag{4.9}$$

where l_i is the distance between successive surface particles i and $i + 1$ in the general displaced surface configuration:

$$l_i^2 = (l_s + x_{i+1} - x_i)^2 + (y_{i+1} - y_i)^2 \tag{4.10}$$

The horizontal-direction periodicity requires that x_{N_s+1}, y_{N_s+1} be identified as x_1, y_1.

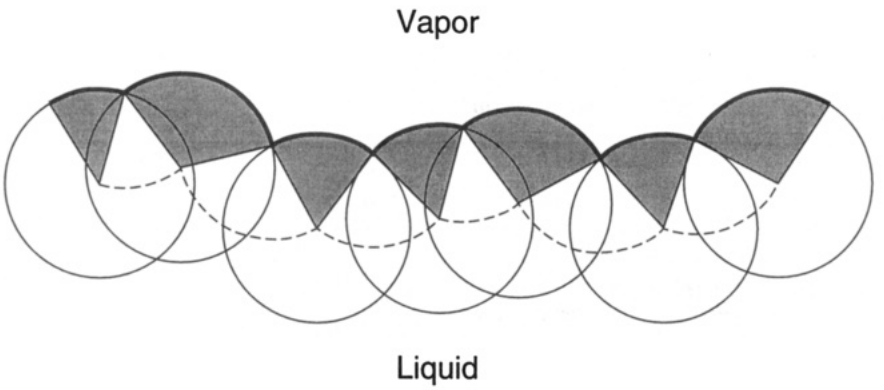

Figure 4. Resolution of area $A_c - A_b$ (between bold and dashed curves) into an alternating sequence of circular sectors. When periodic boundary conditions apply in the horizontal direction, the total areas of shaded and of unshaded sectors are equal.

Upon substituting eq 4.9 into eq 4.8, we obtain

$$Z_N \cong \left[\frac{a\exp(\beta\epsilon)}{\lambda^2\beta\epsilon}\right]^N \sum_{N_s}\left(\frac{\beta\epsilon}{a}\right)^{N_s} \int \mathrm{d}\mathbf{r}_1 \ldots \int \mathrm{d}\mathbf{r}_{Ns} \prod_{i=1}^{N_s} \times$$

$$\exp\left\{-\left(\frac{\beta\epsilon}{\pi}\right)\arccos\left[1 - \frac{(l_s + x_{i+1} - x_i)^2 + (y_{i+1} - y_i)^2}{2R^2}\right]\right\} \tag{4.11}$$

The product form of the integrand would permit straightforward exact evaluation of the multiple integral, using convolution techniques, except for the configurational constraints imposed by definition of the surface particles. However, the low-temperature regime under consideration again comes to the rescue. Surface tension is expected to be large, and the resulting surface stiffness should limit the particle excursions x_i, y_i to small values. Therefore, we can expand the exponent in the integrand of eq 4.11 and drop terms higher than second order:

$$Z_N \cong$$

$$\left[\frac{a\exp(\beta\epsilon)}{\lambda^2\beta\epsilon}\right]^N \sum_{N_s}\left\{\left(\frac{\beta\epsilon}{a}\right)\exp\left[-\left(\frac{\beta\epsilon}{\pi}\right)\arccos\left(1 - \frac{l_s^2}{2R^2}\right)\right]\right\}^{N_s} \times$$

$$\int \mathrm{d}\mathbf{r}_1 \ldots \int \mathrm{d}\mathbf{r}_{N_s} \exp\left\{-\left(\frac{\beta\epsilon}{2\pi l_s R}\right)\left(1 - \frac{l_s^2}{4R^2}\right)^{-1/2} \sum_{i=1}^{N_s}\left[\left(\frac{l_s^2}{4R^2}\right) \times \right.\right.$$

$$\left.\left.\left(1 - \frac{l_s^2}{4R^2}\right)^{-1}(x_{i+1} - x_i)^2 + (y_{i+1} - y_i)^2\right]\right\} \tag{4.12}$$

As we shall confirm momentarily, the high liquid-phase areal density produces a high linear density of surface particles, so that

$$l_s \ll R \tag{4.13}$$

Consequently the x-direction restoring forces are negligibly small compared to those for the y direction. Then aside from the serial ordering of the N_s surface particles, their x-direction motion may be treated as substantially free in eq 4.12. After utilizing (4.13) consistently for other terms in eq 4.12, we arrive at the expression

$$Z_N \cong \left[\frac{a\exp(\beta\epsilon)}{\lambda^2\beta\epsilon}\right]^N \exp\left[-\left(\frac{\beta\epsilon}{\pi R}\right)L_0\right]\sum_{N_s}\frac{1}{N_s!}\left(\frac{\beta\mathrm{e}L_0}{a}\right)^{N_s} \times$$

$$\int \mathrm{d}y_1 \ldots \int \mathrm{d}y_{N_s} \exp\left[-\left(\frac{\beta\epsilon}{2\pi l_s R}\right)\sum_{i=1}^{N_s}(y_{i+1} - y_i)^2\right] \tag{4.14}$$

Notice the automatic appearance of the Boltzmann factor in front of the N_s sum, containing the interface nominal length L_0 times the excess energy per unit length, eq 3.6, for the undisturbed surface.

The normal direction displacement coordinates remaining in Z_N, eq 4.14, determine the capillary waves for the two-dimensional WR model, at least in its low-temperature limiting behavior. To find their expected number and contribution to the surface free energy, we must evaluate the remaining Gaussian integrals. In principle these are constrained by the horizontal periodicity that has been imposed, and by the (virtually) fixed area A_b of the liquid bulk. But in the thermodynamic limit of interest, the N_s relative normal displacements $y_{i+1} - y_i$ may be treated as independent variables. Therefore, Z_N finally adopts the form

$$Z_N \cong \left[\frac{a\exp(\beta\epsilon)}{\lambda^2\beta\epsilon}\right]^N \exp\left[-\frac{\beta\epsilon L_0}{\pi R}\right]\sum_{N_s}\frac{1}{N_s!}\left[\frac{2L_0{}^3\beta\epsilon}{R^3 N_s}\right]^{N_s/2} \tag{4.15}$$

The next task is to identify the maximum term $N_s{}^*$ in the N_s sum. This requires

$$0 = \frac{\partial}{\partial N_s}\ln\left[\frac{1}{N_s!}\left(\frac{2L_0{}^3\beta\epsilon}{R^3 N_s}\right)^{N_s/2}\right] \tag{4.16}$$

which leads to the following result for the linear density of surface particles:

$$\frac{N_s{}^*}{L_0} = \frac{1}{R}\left(\frac{2\beta\epsilon}{e}\right)^{1/3} \tag{4.17}$$

On account of the first of eqs 3.3 this can be reexpressed as follows:

$$l_s{}^* = L_0/N_s{}^* = (eR/2\pi\varrho_1)^{1/3} \tag{4.18}$$

It is usually assumed[5,12] that the short-wavelength cutoff on capillary waves well below the critical point is proportional to the nearest-neighbor spacing in the liquid, which for the present two-dimensional case would require the density factor $\varrho_1{}^{-1/2}$.

However, the naturally appearing surface modes in our analysis are fewer in number and produce instead the factor $\varrho_l^{-1/3}$, though admittedly the model and its low-temperature limit are rather special. Nevertheless, this legitimately raises questions about the validity of short-wavelength cutoff criteria employed in the usual capillary wave treatments.

By retaining only the $N_s = N_s^*$ term in expression (4.15), ln Z_N can be evaluated correctly through the requisite thermodynamic order. The resulting free energy contains both bulk-phase contributions and an interfacial free energy proportional to the nominal interface length L_0. This permits us to identify the line tension γ for the interface:

$$\gamma \cong \frac{\epsilon}{\pi R} - \frac{3}{2R}\left(\frac{2\epsilon}{e\beta^2}\right)^{1/3} \tag{4.19}$$

The temperature-independent leading term is nothing but the surface excess energy identified previously in eq 3.6. The negative second term is the contribution of independent capillary waves.

Had it been possible to avoid the low-temperature approximations that were invoked in our analysis above, eq 4.19 surely would have contained higher-order terms in temperature. One can reasonably expect these higher-order terms to be significant on account of the large density change in the liquid phase that accompanies its heating up to the critical point (estimated earlier in eq 3.2), with the complicating features of voids in the bulk liquid and of interfacial overhangs or protrusions. Support for that expectation comes by observing that expression 4.19 vanishes linearly at

$$\begin{aligned}\beta\epsilon &= (27\pi^3/4e)^{1/2} \\ &= 8.7746... \end{aligned} \tag{4.20}$$

nearly a factor of 2 lower in temperature than was previously estimated for the critical point, where the surface tension actually should go to zero.

V. Intrinsic Density Profile

By setting all capillary wave mode amplitudes to zero (*i.e* all $y_i = 0$), the particle distribution through the interface by a natural definition becomes the intrinsic density profile, to be denoted now by $\varrho_{in}(y)$. As a result of the foregoing, it can be resolved into surface and bulk particle contributions:

$$\varrho_{in}(y) = (N_s^*/L_0)\,\delta(y) + \varrho_{in,b}(y) \tag{5.1}$$

The bulk particle contribution will be a continuous function of y subject to the obvious limit ϱ_l as $y \to -\infty$. We continue to adhere to the low-temperature regime for which we must take

$$\varrho_{in,b}(y) = 0 \qquad (y \geq 0) \tag{5.2}$$

Evaluation of $\varrho_{in,b}$ proceeds most easily by using the identity

$$d\varrho_{in,b}(y)/dy = -\varrho_l Q(y) \tag{5.3}$$

where $Q(y)$ is the normalized probability distribution for the normal-direction position of the scalloped bulk-particle boundary (dashed curve in Figures 2–4), when all surface particles lie on the line $y = 0$. Recall that the tangential (x) direction motion of surface particles is essentially free in the low-temperature limit, aside from their serial ordering. The depth of penetration into the bulk liquid of the radius R circular arc connecting a successive pair of surface particles depends on their tangential separation l, and so we must account for the fact that the normalized distribution of these l values, with mean l_s^*, has the usual form for nearest neighbors on a line,[29]

$$P(l) = (1/l_s^*)\exp(-l/l_s^*) \tag{5.4}$$

We next obtain $p(y|l)$, the normalized distribution of y for a single circular arc spanning an interval of length l. It is consistent to replace that circular arc by its quadratic approximation, a parabola, since l is virtually always much smaller than R. This leads directly to a simple expression,

$$\begin{aligned} p(y|l) &= 0 \qquad (y < -l^2/8R) \\ &= \frac{(2R)^{1/2}}{l[y + (l^2/8R)]^{1/2}} \qquad (-l^2/8R < y \leq 0) \\ &= 0 \qquad (0 < y) \end{aligned} \tag{5.5}$$

Results (5.4) and (5.5) now can be combined to produce an expression for $Q(y)$. After taking due account of the fact that intervals l must be weighted proportionately to their lengths, we find for $y \leq 0$

$$\begin{aligned} Q(y) &= \int_0^\infty dl\,(l/l_s^*)\,P(l)\,p(y|l) \\ &= \frac{4R}{(l_s^*)^2}K_0\left[\frac{(8R|y|)^{1/2}}{l_s^*}\right] \end{aligned} \tag{5.6}$$

Here K_ν is the order-ν modified Bessel function of the second kind.[30] One easily verifies that Q is indeed properly normalized.

The next step is to integrate eq 5.3, using the specific Q form just derived. The result is the following ($y \leq 0$):

$$\varrho_{in,b}(y) = \varrho_l\left\{1 - \frac{(8R|y|)^{1/2}}{l_s^*}K_1\left[\frac{(8R|y|)^{1/2}}{l_s^*}\right]\right\} \tag{5.7}$$

The intrinsic density profile is plotted in reduced form in Figure 5. It may be of interest to note that for large negative y, eq 5.7 indicates the following asymptotic approach to the bulk phase density:

$$\varrho_{in,b}(y) \sim \varrho_l\left\{1 - \left(\frac{\pi}{2}\right)^{1/2}\left[\frac{(8R|y|)^{1/2}}{l_s^*}\right]^{1/2}\exp\left[-\frac{(8R|y|)^{1/2}}{l_s^*}\right]\right\} \tag{5.8}$$

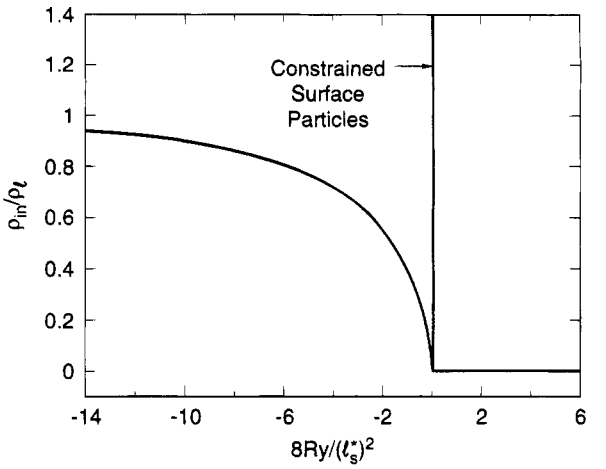

Figure 5. Intrinsic density profile for the two-dimensional WR model at low temperature. Surface particles contribute a delta function at the origin.

Owing to the presence of the surface particle delta function in eq 5.1, the intrinsic density profile is a nonmonotonic function of y. This departs from the usual expectation of a rapidly varying, but monotonic, profile shape. Note, however, that an analogous Kronecker delta would appear in the low-temperature description of the two-dimensional Ising model, where the intrinsic profile would be keyed to the unique "long contour".[31] Furthermore, even the continuous part due to the bulk particles shown in Figure is quite asymmetric about its midpoint $\varrho_l/2$. Finally, the liquid-side asymptotic decay rate exhibited in eq 5.8 is slower than the conventionally expected simple exponential.

The decline of $\varrho_{in,b}(y)$ below ϱ_l for $y \leq 0$ amounts to a surface deficit of particles, the number per unit interface length of which is found to be $(e/4\pi)(N_s^*/L_0)$. This amount is comparable to, but quantitatively less than, the lineal density of surface particles N_s^*/L_0. This implies that the Gibbs equimolar dividing line[32] for ϱ_{in} is displaced from $y = 0$ toward the vapor ($y > 0$) by a distance

$$\Delta = \pi(2/e)^{1/3}[1 - (e/4\pi)](\beta\epsilon)^{-2/3}R \tag{5.9}$$

VI. Surface Tension Dispersion

Use the N_s^* surface particle normal-direction displacements y_j to define the quantities

$$F(k) = (2/N_s^*)\sum_{j=1}^{N_s^*} \cos(kjl_s^*)y_j$$

$$G(k) = (2/N_s^*)\sum_{j=1}^{N_s^*} \sin(kjl_s^*)y_j \tag{6.1}$$

These linear relations can be inverted. For the assumed tangential-direction periodic boundary conditions, k will be restricted to the values

$$k = 0, 2\pi/L_0, 4\pi/L_0, ..., (N_s^* - 1)\pi/L_0 \quad (N_s^* \text{ odd})$$

$$= 0, 2\pi/L_0, 4\pi/L_0, ..., N_s^*\pi/L_0 \quad (N_s^* \text{ even}) \tag{6.2}$$

Then we have

$$y_j = \sum_k [F(k) \cos(kjl_s^*) + G(k) \sin(kjl_s^*)] \tag{6.3}$$

where the sum spans the appropriate set (6.2). In this expression it is clear that the $F(k)$ and $G(k)$ are the capillary wave amplitudes.

Examination of the partition function in the earlier eq 4.15 shows that the surface particles experience a quadratic potential energy:

$$\Phi_s = \left(\frac{\epsilon}{2\pi l_s^* R}\right)\sum_{j=1}^{N_s^*} (y_{j+1} - y_j)^2 \tag{6.4}$$

Upon inserting expressions 6.3, this interaction adopts the form

$$\Phi_s = \left(\frac{\epsilon(N_s^*)^2}{2\pi R L_0}\right)\sum_k [1 - \cos(kl_s^*)][F^2(k) + G^2(k)] \tag{6.5}$$

displaying independent quadratic contributions from each of the N_s^* capillary wave normal modes.

Consider a single mode, say the cosine case for some $k > 0$. The formal interface length increment δL_0 attributable to this mode can immediately be calculated from the corresponding continuous perturbed boundary position

$$y(x) = F \cos(kx) \tag{6.6}$$

by means of the usual length formula:

$$\delta L_0 = \int_0^{L_0} dx[1 + (y')^2]^{1/2} - L_0$$

$$= F^2k^2L_0/4 + O(F^4) \tag{6.7}$$

The associated energy expenditure can be written as $\gamma_0(k)\,\delta L_0$, where $\gamma_0(k)$ is a "bare" surface tension for the given wavelength. By comparing eqs 6.5 and 6.7 we find

$$\gamma_0(k) = (\epsilon/\pi R)f(kl_s^*)$$

$$f(u) = (2/u^2)(1 - \cos u) \tag{6.8}$$

The function $f(u)$ declines monotonically from 1 at the origin to $4/\pi^2 = 0.405\,28...$ at $u = \pi$, the upper limit for the capillary waves. Notice that $\gamma_0(0+)$ is nothing but the excess potential per unit boundary length for a flat interface, eq 3.6. Short-wavelength interface disturbances by contrast incur a reduced surface energy, *i.e.*, reduced bare surface tension.

VII. Discussion

The advantage of studying the two-dimensional WR model is clear: in its low-temperature regime various simplifications permit a rather complete analysis to be carried out and several important results to be extracted. The latter include unambiguous enumeration of surface capillary modes and their upper wavelength cutoff, identification of bare surface tension dispersion, and explicit evaluation of an intrinsic density profile that is nonmonotonic. Of course the model and its temperature restriction are very special circumstances, so it must be asked if these results have significant implications for the general theory of liquid−vapor interfaces.

It was remarked above that a major physical shortcoming of the WR model family is the absence of short-range particle repulsions. This can easily be rectified, say by adding a sum of hard-sphere (or hard-disk) pair potentials to the WR interaction. If the collision diameter of these core interactions were small compared to the length R, it should be possible at least in part to account for the effects of this perturbation in a variety of standard methods, including Mayer cluster theory.[33] Unfortunately, the introduction of hard cores blocks use of the strategy described above, where temperature is a natural small parameter. The low-temperature phase now is crystalline, not liquid, and its density is strictly bounded due to hard core exclusions. Nevertheless, for small cores it seems reasonable to expect that near the liquid's low freezing temperature surface modes still could be identified, and the intrinsic density profile would continue to exhibit nonmonotonic shape.

In order to extend the study to somewhat higher temperatures, several features require attention. The nonvanishing vapor density and gaps in the bulk liquid phase become important in principle, but once again these should only require renormalization of quantities appearing in the low-temperature regime. The presence of protrusions (as shown in Figure 2) may pose technical problems, but it appears that they would be integrated out to provide additional renormalization of the motion of the primary surface particles (those in Figure 2 whose centers lie on the dashed curve).

The natural sequential ordering of surface particles along the one-dimensional interface is a convenient characteristic in

analyzing the two-dimensional WR model, since any surface configuration can then be referred to the unique regular reference array. The corresponding three-dimensional WR model is more problematic. While surface particles can still be identified as those contributing parts of their radius R spheres to the outer boundary of the liquid, the choice of a regular reference site lattice is not unique, and a continuum treatment for the interfacial free energy such as that given in the Appendix necessarily involves as-yet undetermined constant factors of order unity in the interfacial free energy. Whatever the specific choice, we believe on the basis of general statistical–thermodynamic arguments given in the Appendix that extension of present results to the three-dimensional case would inevitably lead to an upper cutoff on surface mode $|\mathbf{k}|$'s that is proportional to $\varrho_l^{1/4}$ in the low-temperature regime. Furthermore, a nonmonotonic intrinsic density profile must emerge from the analysis, a feature that occasionally has been anticipated in prior studies.[34,35]

The principal conclusion to be drawn from the present work is that the general theory of the liquid–vapor interface still lacks an important ingredient. It offers no general rule for the full separation of degrees of freedom into surface modes and bulk modes. Consequently, it has no general procedure for precise enumeration of the surface (capillary wave) modes and thus no unambiguous criterion for location of an upper wave vector cutoff. Unless this need is fulfilled, it will remain uncertain in general how to determine intrinsic density profiles, presuming they are to be defined as the interfacial density distribution with all surface modes constrained to vanishing amplitude. It will also remain uncertain whether nonmonotonicity must be accepted as a universal characteristic of intrinsic density profiles. We hope the present paper will stimulate the required strengthening of the general theory.

Appendix

In this Appendix we present an alternate approach that can be used to derive many of the results in the main text. The method is more heuristic but can be used to generalize those results to arbitrary dimensions d.

The basic idea is very simple. Since the surface particles can be precisely defined in the low-temperature limit, we can calculate a "surface phase" partition function by integrating over all permitted motions of the surface particles. This essentially involves calculating the free energy of long-wavelength distortions of a nominally flat interface, and we can use methods similar to those in standard capillary wave theory.[1,11,21,23] This surface phase is in equilibrium with coexisting bulk liquid and vapor phases. The average density of surface particles can be determined by requiring equality of the chemical potentials calculated from the surface and bulk partition functions.

To implement this program let us first calculate the coexisting bulk phase densities and the chemical potential at very low temperatures. In the dilute vapor phase the potential energy (2.1) vanishes and the partition function is simply that of a classical ideal gas:

$$Z_v = \frac{V_v^{n_v}}{\lambda^{dN_v} N_v!} \tag{A.1}$$

Here V_v is the d-dimensional volume of the ideal gas. As discussed in the text, particles in the bulk liquid phase also behave ideally, while moving in a uniform potential proportional to the covered volume as in eq 2.1; thus

$$Z_l = \frac{V_l^{N_l} \exp[-(\beta\epsilon/v)(V_l - N_l v)]}{\lambda^{dN_l} N_l!} \tag{A.2}$$

Here v is the volume of the WR sphere. Two-phase coexistence requires equality of the pressure, calculated from $\partial \ln Z/\partial V$, and the chemical potential, calculated from $-\partial \ln Z/\partial N$. Thus from (A.1) and (A.2) we find

$$-\beta\epsilon/v + \varrho_l = \varrho_v \tag{A.3}$$

and

$$-\beta\epsilon + \ln(\varrho_l\lambda^3) = \ln(\varrho_v\lambda^3) \tag{A.4}$$

Thus the coexisting densities are

$$\varrho_l = \frac{\beta\epsilon}{v(1 - e^{-\beta\epsilon})} \tag{A.5}$$

and

$$\varrho_v = \frac{\beta\epsilon e^{-\beta\epsilon}}{v(1 - e^{-\beta\epsilon})} \tag{A.6}$$

To lowest order these agree with eq 3.3. This shows the consistency of our ideal gas picture for the bulk phases at sufficiently low temperatures in the WR model. Henceforth, we ignore terms of $O(e^{-\beta\epsilon})$, setting ϱ_v to zero. Note from (A.3) that the liquid phase then has zero pressure. The chemical potential from (A.4) is

$$\beta\mu = \ln(\varrho_l\lambda^d) - \beta\epsilon = \ln(\beta\epsilon\lambda^d/v) - \beta\epsilon \tag{A.7}$$

Finally, a_l, the Helmholtz free energy per particle for the bulk liquid, is given by $\beta a_l = \beta\mu - \beta p/\varrho_l$. Since $p = 0$ in this case, we have

$$\beta a_l = \beta\mu = \ln(\varrho_l\lambda^d) - \beta\epsilon \tag{A.8}$$

Now we calculate the surface partition function, Z_s. This clearly involves the energetics of the N_s surface particles confined to the surface strip. Using capillary wave theory, we expect that long-wavelength fluctuations of the strip are controlled by the surface tension times the change in area, and the constraining effects of surface tension become increasingly important at low temperatures. While in general there is some debate about what is the proper (bare or renormalized) surface tension to use in capillary wave theory,[1,11,14,21] for our purposes here it is clearly sufficient to use the limiting low-temperature value

$$\gamma_0 = \epsilon R/v \tag{A.9}$$

as in eq 3.6. Let α_0 be the nominal $d' \equiv d - 1$ dimensional surface area (analogous to L_0 in Figure 1). We are primarily interested in determining the surface particle density

$$\varrho_s \equiv N_s/\alpha_0 \tag{A.10}$$

and the associated length scale

$$l_s \equiv \varrho_s^{-1/d'} \tag{A.11}$$

as in (4.2).

Thus it is plausible that the surface partition function can be written as

$$Z_s = (\lambda^{dN_s} N_s!)^{-1} \exp(-\beta\epsilon\alpha_0 R/v + \beta\epsilon N_s) \int d\mathbf{r}_1 \ldots \int d\mathbf{r}_{N_s} \times \exp[-\beta\gamma_0 \delta\alpha(\mathbf{r}_1 \ldots \mathbf{r}_{N_s})] \tag{A.12}$$

Here $\delta\alpha$ is the change in area due to motions of the N_s particles, and the integrations are constrained to displacements consistent with the definition of surface particles. The exponential term outside the integral is the energy of the undistorted strip calculated using eq 2.1; note that $\epsilon\alpha_0 R/v = \gamma_0\alpha_0$. Proceeding as in the main text we treat the integrations over the d' transverse components x_i of each position vector r_i as free, and introduce Stirling's approximation. This yields

$$Z_s = (\alpha_0 e/N_s\lambda^d)^{N_s} \exp(-\beta\gamma_0\alpha_0 + \beta\epsilon N_s) \int \dots \int d\{z_i\} \times \exp[-\beta\gamma_0\delta\alpha(\{z_i\})] \quad (A.13)$$

where z_i is the coordinate normal to the interface for particle i and $d\{z_i\}$ denotes integration over the set $\{z_i\}$ of all z coordinates. In the near-continuum limit, the distortions of the interface implied by a particular choice of the $\{z_i\}$ can be described using a single-valued function $z(x)$ giving the "height" of the interface at transverse position x. Let us introduce the Fourier series

$$z(x) = \frac{1}{N_s^{1/2}} \sum_q^{q_{max}} \hat{z}(q) e^{iqx} \quad (A.14)$$

where the sum is over a set of N_s wave vectors q whose components satisfy

$$q_j l_s = \frac{2\pi n_j}{\eta_s}; \quad -\eta_s/2 \le n_j \le \eta_s/2 \quad (A.15)$$

for distinct choices of integers n_j. Here $\eta_s \equiv N_s^{1/d'}$ and the sum is cut off at a maximum wave vector $|q_{max}| \approx \pi/l_s$, consistent with the typical spacing l_s of neighboring surface particles. (Our continuum description of interface displacements cannot be extended to smaller length scales.) Then the change in area $\delta\alpha$ can be approximated by[1,11,21]

$$\delta\alpha(\{\hat{z}(q)\}) = {}^1/_2 l_s^{d'} \sum_q^{q_{max}} |\hat{z}(q)|^2 q^2 \quad (A.16)$$

and Z_s becomes

$$Z_s = (\alpha_0 e/N_s\lambda^d)^{N_s} \exp(-\beta\gamma_0\alpha_0 + \beta\epsilon N_s) \int \dots \int d\{\hat{z}(q)\} \times \exp[-\beta\gamma_0\delta\alpha(\{\hat{z}(q)\})] \quad (A.17)$$

noting that the Jacobian of the transformation $\{z_i\} \rightarrow \{\hat{z}(q)\}$ in (A.14) is unity. The steps leading up to (A.17) have been discussed in many papers on capillary wave theory. Introducing dimensionless variables $\bar{q} \equiv q l_s$ and $\bar{z}(\bar{q}) \equiv [\hat{z}(q)/l_s](\beta\gamma_0 l_s^{d'})^{1/2}$ in eq A.17, carrying out the Gaussian integrations, and taking logarithms yields

$$\ln Z_s = -\beta\gamma_0\alpha_0 + \beta\epsilon N_s + N_s \ln\left[\frac{l_s^d e(2\pi)^{1/2}}{\lambda^d(\beta\gamma_0 l_s^{d'})^{1/2}}\right] - N_s c_d \quad (A.18)$$

Here

$$c_d \equiv \int d\bar{q} \ln \bar{q} \quad (A.19)$$

is a constant of $O(1)$ whose precise value is unimportant for what follows, and which in any case cannot be determined reliably using our continuum methods. The integration in (A.19) is restricted to the region $|\bar{q}| \le \pi$.

We are now able to determine the equilibrium values l_s and ϱ_s in terms of ϱ_l by requiring that the chemical potential $\beta\mu_s \equiv -\partial \ln Z_s/\partial N_s$ calculated from (A.18) equals that of the bulk liquid, eq A.7. Recalling the definitions (A.10) and (A.11) we find

$$l_s = (c'_d R/\varrho_l)^{1/(d+1)} \quad (A.20)$$

which generalizes eq 4.19. Here c'_d is a constant of $O(1)$. This is the main result of the Appendix. Note that the usual scaling $l_s \propto \varrho_l^{-1/d}$ would have followed from (A.18) and (A.7) if $\beta\gamma_0 l_s^{d'}$ were of $O(1)$, which is usually the case for real liquids with repulsive cores with radius of order $R \propto l_s$. Using (A.10) and (A.11) we also have

$$\varrho_s \propto (\varrho_l/R)^{(d-1)/(d+1)} \propto \frac{R(\beta\epsilon)^{(d-1)/(d+1)}}{v} \quad (A.21)$$

The approach taken here has much in common with that of section IV in the main text. If we take the appropriate maximum term values for N_b and N_s in eq 4.8 such that $N = N_b + N_s$, Z_N defined there can in essence be written as

$$Z_N = Z_l(N_b;\varrho_l) Z_s(N_s) \quad (A.22)$$

(Recall that a serial order was imposed on the surface particles in section IV.) The notation $Z_l(N_b;\varrho_l)$ in (A.22) emphasizes that the N_b particles have the proper bulk density ϱ_l given by (3.3). In order to extract the capillary wave corrections to the limiting surface tension γ_0 from (A.22) we must remove the bulk contributions proportional to N, i.e., those contained in $Z_l(N;\varrho_l)$. By definition, the surface tension γ then satisfies

$$-\beta\gamma\alpha_0 = \ln\left[\frac{Z_N}{Z_l(N;\varrho_l)}\right] = \ln\left[\frac{Z_l(N_b;\varrho_l)}{Z_l(N;\varrho_l)}\right] + \ln Z_s(N_s) \quad (A.23)$$

Using eqs A.8, A.18, and A.21 in (A.23), we note that the terms involving λ cancel, and after some algebra we are left with

$$\beta\gamma = \beta\gamma_0 - c_1\varrho_s \quad (A.24)$$

where c_1 is a constant of $O(1)$. Using (A.21), we obtain the capillary wave corrections to the surface tension as

$$\gamma = \epsilon R/v - c_2 \frac{R}{v}\left(\frac{\epsilon^{d-1}}{\beta^2}\right)^{1/(d+1)} \quad (A.25)$$

which generalizes eq 4.20.

References and Notes

(1) Rowlinson, J. S.; Widom, B. *Molecular Theory of Capillarity*; Clarendon Press: Oxford, 1982.
(2) Braslau, A.; Deutsch, M.; Pershan, P. S.; Weiss, A. H.; Als-Nielsen, J.; Bohr, J. *Phys. Rev. Lett.* **1985**, *54*, 114.
(3) Beaglehole, D. *Phys. Rev. Lett.* **1987**, *58*, 1434.
(4) Goh, M. C.; Hicks, J. M.; Kemnitz, K.; Pinto, G. R.; Bhattacharyya, K.; Eisenthal, K. B. *J. Phys. Chem.* **1988**, *92*, 5074.
(5) Braslau, A.; Pershan, P. S.; Swislow, G.; Ocko, B. M.; Als-Nielsen, J. *Phys. Rev.* **1988**, *A38*, 2457.
(6) Sanyal, M. K.; Sinha, S. K.; Huang, K. G.; Ocko, B. M. *Phys. Rev. Lett.* **1991**, *66*, 628.
(7) Schmidt, J. W.; Moldover, M. R. *J. Chem. Phys.* **1993**, *99*, 582.
(8) Ocko, B. M.; Wu, X. Z.; Sirota, E. B.; Sinha, S. K.; Deutsch, M. *Phys. Rev. Lett.* **1994**, *72*, 242.
(9) Fisk, S.; Widom, B. *J. Chem. Phys.* **1969**, *50*, 3219.
(10) Wertheim, M. S. *J. Chem. Phys.* **1976**, *65*, 2377.
(11) Weeks, J. D. *J. Chem. Phys.* **1977**, *67*, 3106.
(12) Weeks, J. D. *Phys. Rev. Lett.* **1984**, *52*, 2160.
(13) Kaiser, R. F. *Phys. Rev.* **1986**, *A33*, 1948.
(14) Gelfand, M. P.; Fisher, M. E. *Physica A* **1990**, *166*, 1.
(15) Bonn, D.; Wegdam, G. H. *J. Phys. I (Fr)* **1992**, *2*, 1755.

(16) Widom, B.; Rowlinson, J. S. *J. Chem. Phys.* **1970**, *52*, 1670.
(17) Leng, C. A.; Rowlinson, J. S.; Thompson, S. M. *Proc. R. Soc. London* **1976**, *A352*, 1.
(18) Leng, C. A.; Rowlinson, J. S.; Thompson, S. M. *Proc. R. Soc. London* **1977**, *A358*, 267.
(19) van der Waals, J. D. *Verhandel. Konink. Akad. Weten., Amsterdam (Sect. 1)* **1893**, *1*, No. 8, 56; English translation: *J. Stat. Phys.* **1979**, *20*, 197.
(20) van der Waals, J. D. *Z. Phys. Chem.* **1894**, *13*, 675.
(21) Buff, F. P.; Lovett, R. A.; Stillinger, F. H. *Phys. Rev. Lett.* **1965**, *15*, 621.
(22) Abraham, D. B. *Physica* **1991**, *A177*, 421.
(23) Bedeaux, D.; Weeks, J. D. *J. Chem. Phys.* **1985**, *82*, 972.
(24) Ruell, D. *Statistical Mechanics*; Benjamin: New York, 1969; Chapter 3.
(25) Peierls, R. F. *Phys. Rev.* **1958**, *54*, 918.
(26) Ref 1, pp 151–159.
(27) Fisher, M. E. *Rev. Mod. Phys.* **1974**, *46*, 597.
(28) Huang, K. *Statistical Mechanics*, Wiley: New York, 1963; p 372.
(29) Kendall, M. G.; Moran, P. A. P. *Geometrical Probability*; Hafner: New York, 1963; p 27.
(30) Abramowitz, M.; Stegun, I. A. *Handbook of Mathematical Functions*; NBS Applied Mathematics Series No. 55; U.S. Government Printing Office: Washington, DC, 1968; pp 374–378.
(31) Bricmont, J.; Lebowitz, J. L.; Pfister, C. E. *J. Stat. Phys.* **1981**, *26*, 313.
(32) Gibbs, J. W. *Scientific Papers*; Dover: New York, 1961; Vol. 1, p 234.
(33) Mayer, J. E.; Mayer, M. G. *Statistical Mechanics*; Wiley: New York, 1940; Chapter 13.
(34) Stillinger, F. H. *Int. J. Quantum Chem.* **1982**, *16*, 137.
(35) Stillinger, F. H. *J. Chem. Phys.* **1982**, *76*, 1087.

JP9416836